Applied Catalysis B: Environmental 196 (2016) 68–76

Contents lists available at ScienceDirect

Applied Catalysis B: Environmental

journal homepage: www.elsevier.com/locate/apcatb

Low temperature atomic layer deposition of ZnO: Applications in photocatalysis

Alessandro Di Mauro[a,*], Maria Cantarella[a,b], Giuseppe Nicotra[c], Vittorio Privitera[a], Giuliana Impellizzeri[a]

[a] CNR-IMM, Via S. Sofia 64, 95123 Catania, Italy
[b] Department of Physics and Astronomy, University of Catania, Via Santa Sofia 64, 95123 Catania, Italy
[c] CNR-IMM, Z.I. VIII Strada 5, 95121 Catania, Italy

ARTICLE INFO

Article history:
Received 25 February 2016
Received in revised form 27 April 2016
Accepted 8 May 2016
Available online 11 May 2016

Keywords:
ZnO film
ALD
Low temperature
Photocatalysis
Polymer

ABSTRACT

This work reports on the ZnO thin films obtained by atomic layer deposition (ALD), at a deposition temperature down to 40 °C. The crystallinity of the material as a function of the film thickness and the deposition temperature was investigated. The photocatalytic performance was evaluated by the degradation of methylene blue (MB) dye in water under UV light irradiation. The effect of the film thickness and the deposition temperature on the photocatalysis was deeply elucidated. Once the optimized conditions (in terms of thickness and temperature) were found, the ALD process was transferred on a flexible polymeric substrate: polyethylene naphthalate (PEN). The photo-activity of the flexible materials was evidenced by the degradation of MB and phenols in water. The results demonstrate that low temperature growth by ALD can be fruitfully applied to synthesize flexible materials that can found applications in photocatalysis.

1. Introduction

Zinc oxide (ZnO) has rapidly attracted increased attention in the last few years. It is a prospective material for several applications, such as for UV light emitters, gas sensors, piezoelectric transducers, transparent electronics, solar cells and photocatalysis [1–5]. This variety of applications derives from the specific properties of ZnO. It is a wide band-gap semiconductor (E_g ~3.3 eV at 300 K); it is harmless; it has a high thermal and chemical stability; it has a relatively low-cost; it is simple to grow, resulting in a potentially low cost for ZnO-based devices.

The success of ZnO for many applications is associated to the flexible feature of the substrate. For this reason, many researcher groups are studying advanced methods effective in the deposition of ZnO on thermally-fragile polymer substrates.

The most common methods used to grow ZnO thin films are pulsed laser deposition [6], and radio-frequency magnetron sputtering [7]. It is worth noting that radio-frequency magnetron sputtering, when applied at low temperature, requires post-growth annealing [7], often incompatible with polymeric substrates. In this context, a promising deposition technique is the atomic layer deposition (ALD), because of its unique benefits: homogeneity, conformity, density. ALD is highly reproducible and easily scalable to industrial process level [8]. The vast majority of ALD processes occur at substrate/reactor temperature exceeding 200 °C. However, deposition at low temperature, the so-called low-temperature ALD (LT-ALD), has recently attracted the interest of many of research groups, paving the way toward exciting novel applications. Quite few papers report on ZnO films fabricated by LT-ALD [9–12]. Guziewicz et al. demonstrated the high quality, in terms of optical and electrical properties, of ZnO films deposited by thermal ALD from 90 to 200 °C [10]. Another paper reports on plasma-enhanced ALD of ZnO from 25 to 120 °C, evidencing how, with increasing temperature, the film purity, refractive index, and electrical conductivity increase, before saturating at constant values within the ALD windows (85–120 °C) [11]. Interestingly there is not, to our knowledge, any study focused on LT-ALD for photocatalytic applications. In the field of water purification by photocatalysis, the employment of photocatalytic coatings, for example on plastic bottles, represents one of the step forward the industrial exploitation [13].

* Corresponding author.
E-mail addresses: alessandro.dimauro@ct.infn.it (A. Di Mauro), maria.cantarella@ct.infn.it (M. Cantarella), giuseppe.nicotra@imm.cnr.it (G. Nicotra), vittorio.privitera@imm.cnr.it (V. Privitera), giuliana.impellizzeri@ct.infn.it (G. Impellizzeri).

http://dx.doi.org/10.1016/j.apcatb.2016.05.015
0926-3373/

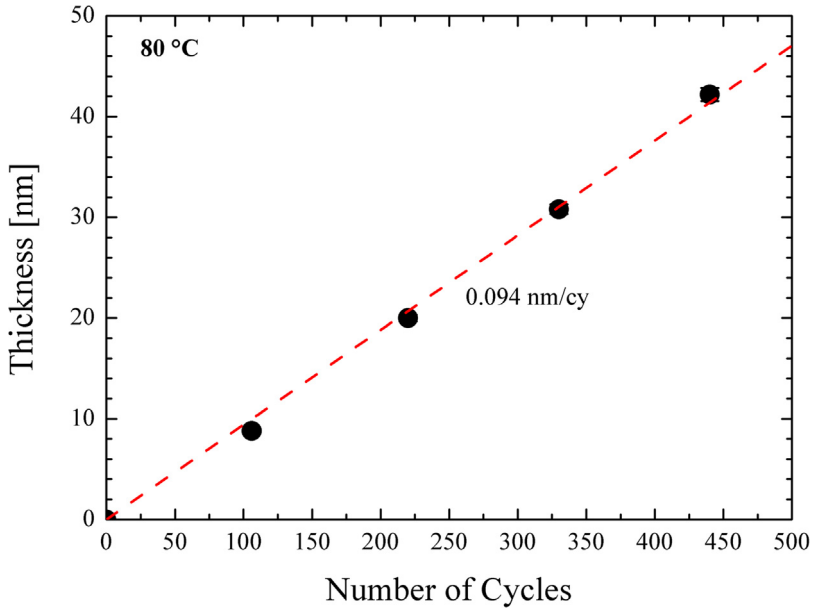

Fig. 1. Film thickness of ZnO deposited by ALD at 80 °C as a function of the number of the ALD cycles (closed circles). Film growth rate was extrapolated by the linear fit of the experimental data (dashed line).

In this paper, we present a systematic study of ZnO films deposited by LT-ALD, from 40 to 120 °C. The growth rate together with the crystallinity of the materials were monitored. In addition, the photocatalytic performance of the films was investigated, by the degradation of methylene blue dye in aquatic environment, as a function of the deposition temperature and the film thickness. Finally, the deposition process was repeated with polyethylene naphthalate (PEN), a widespread polyester with significant performance properties. The photocatalytic performances of these films were also tested towards the degradation of dyes and phenols, showing promising behaviours.

2. Experimental

2.1. Preparation of ZnO thin films by ALD

ZnO films with different thicknesses (from ~9–48 nm) were deposited by ALD using the Picosun R-200 Advanced reactor. During the deposition the temperature was fixed at 40, 80 or 120 °C. 8 inches silicon wafers were used as substrates; few depositions were performed also on quartz substrates for optical measurements, and on PEN, in order to transfer the process on a flexible support. Diethyl zinc (DEZ, purity 100%) and de-ionized water were used as precursors, while N_2 was used as carrier and purge gas (purity ≥ 99.999%). The pulse and purge time were kept constant at 0.1/3/0.1/5 s for DEZ/N_2/H_2O/N_2. The film thickness was evaluated by the M-2000 spectroscopic ellipsometer by Woollam, equipped with a mapping stage, by applying a Cauchy model to 317 points for each 8″ wafer in the 400–1700 nm range. The uniformity of the films was lower than 2% on 8″ wafers. The PEN used for this study had a thickness of 0.13 mm.

2.2. Characterization of ZnO thin films

The morphology of the surface was explored by scanning electron microscopy (SEM), with a field emission Zeiss Supra 25 microscope. The crystallinity of the films was investigated by X-ray diffraction (XRD) analyses with a Bruker D-500 diffractometer (detector scan mode) at 0.5° angle of incidence, and 2θ from 20 to 50°. The XRD spectra were analysed by the Bruker software suite, including ICSD structure database.

The UV–vis optical characterization was obtained by extracting both the normal transmittance (T) and the 5° reflectance (R) spectra in the 200–1000 nm wavelength range, by using a Perkin-Elmer Lambda 35 UV/VIS/NIR spectrophotometer.

2.3. Photocatalytic activity under UV light irradiation

The photocatalytic activity of the investigated films was tested by the degradation of methylene blue (MB) dye in water. Before any measurement, the samples were irradiated by an UV lamp for 60 min in order to remove the hydrocarbons from the sample [14]. The samples, 1 cm × 1 cm in size, were thereafter immersed in a 2 ml solution containing MB and de-ionized water, with a starting concentration of MB of 1.5×10^{-5} M. The measurements were performed at a fixed pH value (7.5), using NaOH to control the pH value. The MB solution containing the ZnO sample was irradiated by an UV lamp (350–400 nm wavelength range) with an irradiance of 2 mW/cm^2. The irradiated solution was measured at regular time intervals, up to 4 h, with an UV–vis spectrophotometer (Lambda 35, Perkin-Elmer) in a wavelength range of 500–800 nm. The degradation of MB was evaluated by the absorbance peak at 664 nm in the Lambert-Beer regime [15]. The decomposition of the MB dye in the absence of any photocatalyst materials was checked as a reference. Control experiments in the dark for 1 h were conducted to clarify the contribution of the adsorption of the MB on the beaker surface and on the sample surface.

The photocatalytic activity of the ZnO layers was also tested for the degradation of phenols, employing the same procedure as described above for the MB degradation. The starting solution included phenols in de-ionized water, with a phenol concentration of 1.38 mg/l. The variation of the concentration of phenols was measured spectrophotometrically (Hach DR 3900 spectrophotometer), using LCK345 cuvette tests.

3. Results and discussions

With the main aim of investigating the LT-ALD, we grew ZnO films at a deposition temperature of 80 °C, with different thick-

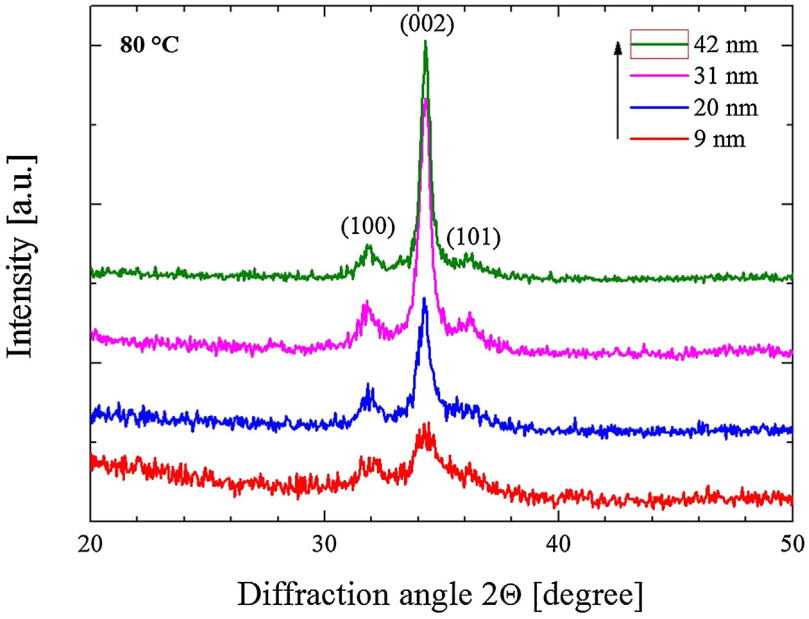

Fig. 2. XRD patterns of ZnO films deposited by ALD at 80 °C with different thickness (between 9 and 42 nm).

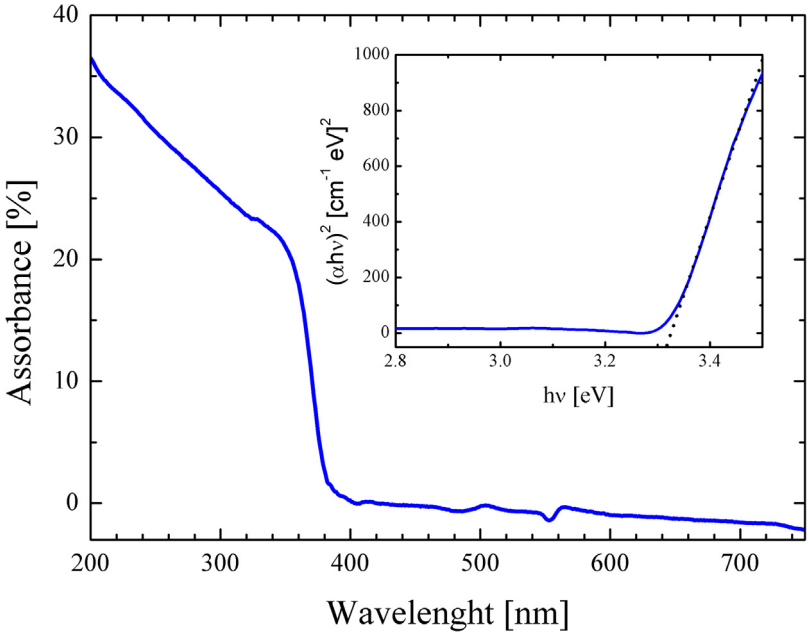

Fig. 3. Absorbance spectrum of the ZnO film 20 nm thick deposited by ALD at 80 °C. The inset reports the Tauc plot (continuous line) togheter with the linear fit (dotted line).

nesses: 9, 20, 31 and 42 nm (obtained by varying the number of the ALD cycles). Fig. 1 shows the film thickness of ZnO as a function of the number of the ALD cycles (circles). The error in the evaluation of the thickness, within the 2%, was the standard deviation deduced by the ellipsometry measurements (317 measurements on each 8″ wafer) and is within the symbols. The trend of the film thickness was linear with respect to the number of the ALD cycles, which indicates a self-limiting growth of the films. The linear fit of the experimental data (reported in Fig. 1 as a dashed line) gives a growth rate of 0.094 nm per cycle for ZnO deposited at 80 °C.The structural analyses performed by XRD can be seen in Fig. 2. All of the ZnO films deposited at 80 °C were polycrystalline, despite the low temperature. The diffraction patterns show well-defined Bragg peaks corresponding to the planes (100), (002), (101); this also confirms the wurtzite crystal structure of the whole set of samples. The strong signals at 34.5° indicate a preferential growth along the (002) direction, because the *c*-plane perpendicular to a substrate is the most densely packed and thermodynamically favourable plane in the wurtzite structure [16]. The increase of the diffraction peak intensity with the thickness is an indication of the enhanced crystallinity of the films within a specific thickness range [10,16]. The optical properties of the investigated samples were analysed by optical characterization. In Fig. 3, as an example, the absorbance for the ZnO film, 20 nm thick, deposited at 80 °C is reported. The absorbance (A) was obtained by the transmittance (T) and reflectance (R) measured spectra, in accordance with the following equation: A% = 100% – T% – R%. The film shows the typical optical absorption in the UV part of the spectrum, for wavelengths shorter than ~390 nm (continuous line in Fig. 3). The small step observed at 326 nm is due to the change of the lamp during the spec-

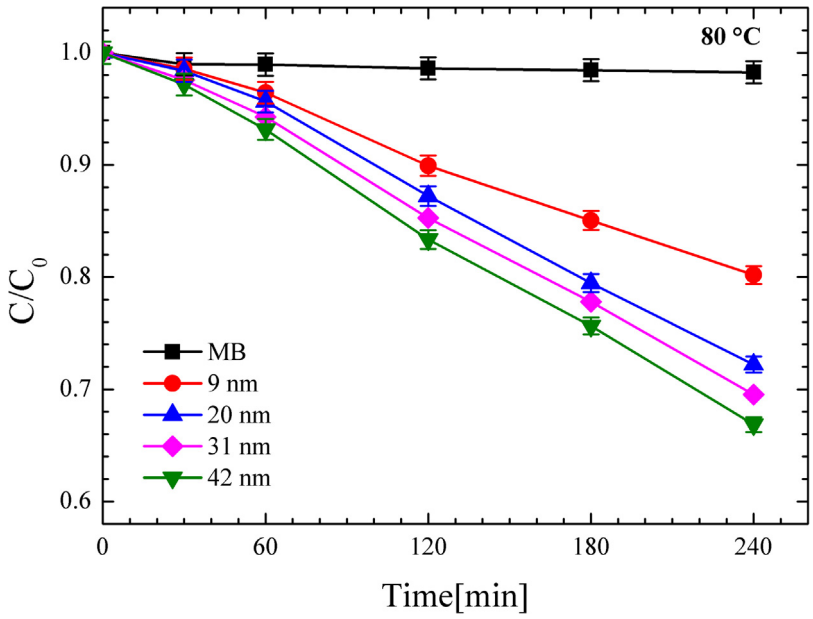

Fig. 4. MB photo-degradation under UV irradiation for five samples: MB (squares), MB with the ZnO thin films: 9 nm thick (circles), 20 nm thick (up triangles), 31 nm thick (diamonds), 42 nm thick (down triangles).

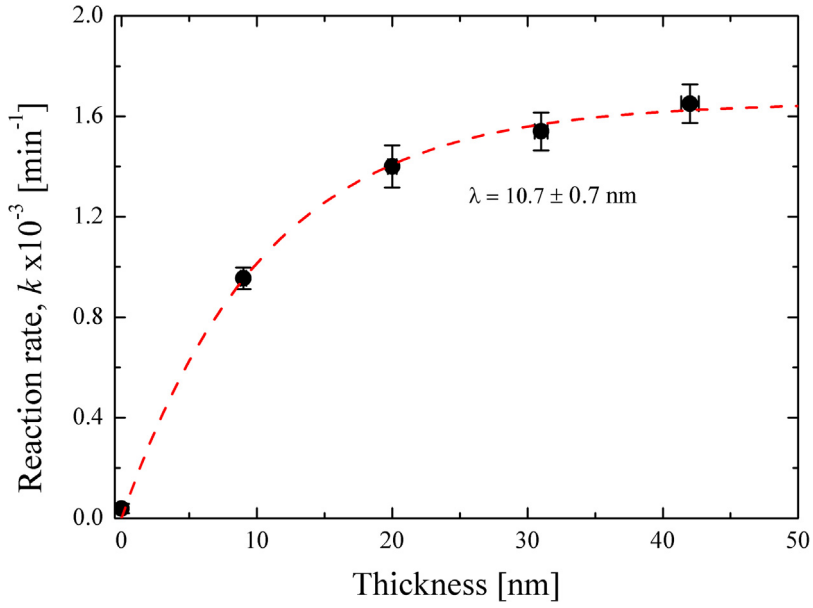

Fig. 5. Reaction rate, k, plotted as a function of the film thickness (circles). The best fit of the experimental data is reported with dashed line. The extrapolated charge diffusion length, λ, is pinned, too.

trophotometric measurements. The optical spectrum was analysed by the Tauc model, which describes the light absorption process in amorphous semiconductors [17]. The pertinence of the model was demonstrated also for polycrystalline semiconductors, and in particular for ZnO [18]. They showed that the optical absorption strength depends on the difference between the photon energy and the band-gap energy as follows:

$$(\alpha h\nu)^{1/n} = B(h\nu - E_g) \quad (1)$$

where α is the absorption coefficient, h is the Plank's constant, ν is the photon's frequency, B is a proportionality constant, E_g is the optical band-gap of the material. The value of the exponent denotes the nature of the electronic transition, and n is 1/2 for direct allowed transitions, which is the case of ZnO [1]. The absorption coefficient was extracted from the transmittance (T) and reflectance (R) measurements by using the following equation:

$$\alpha = \frac{1}{d} \ln \frac{T_Q(1 - R_S)}{T_S} \quad (2)$$

where d is the thickness of the film; the subscripts Q and S refer to the quartz and the sample, respectively. By plotting $(\alpha h\nu)$ [2] versus $h\nu$ (i.e. Tauc plot) and using a linear fit, E_g can be extracted, consisting in the intercept of the linear fit with the abscissa axis. The inset of Fig. 3 reports the Tauc plot of the ZnO film together with the linear fit (reported with dotted line) which gave an energy gap of 3.3 eV, in perfect agreement with the values reported in the literature for ZnO [1–3].

The photocatalytic activity of ZnO films deposited at 80 °C was tested by the degradation of MB solution. The first test was per-

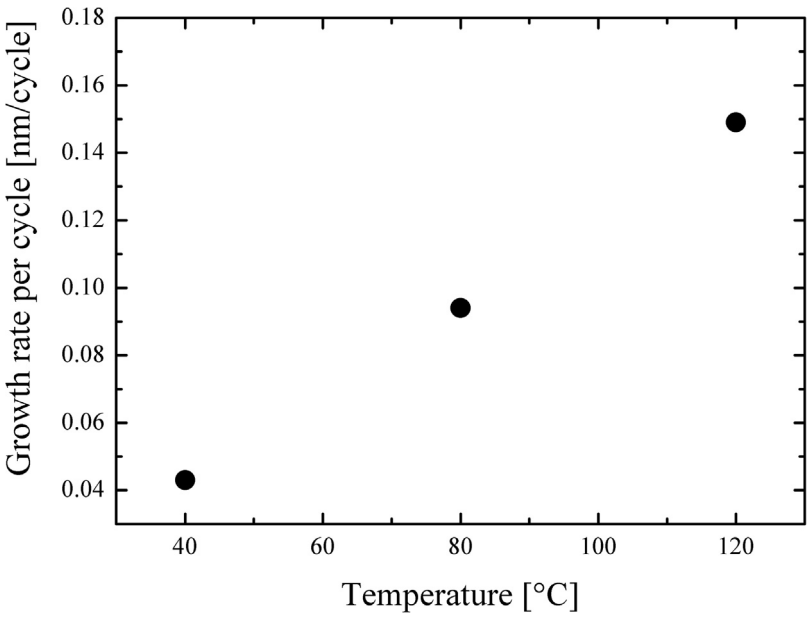

Fig. 6. Growth rate per cycle for ZnO plotted as a function of the ALD deposition temperature (circles).

formed under dark conditions for 1 h, in order to evaluate the degree of adsorption of MB on the beaker walls and on the sample surfaces. The beaker walls showed an adsorption of ~1% (this data was deduced by the use of a beaker only containing the MB solution). The samples showed an adsorption of ~1% (reaching this maximum value after 30 min). The latter result indicates that the investigated materials exhibit a negligible adsorption of MB, since the adsorption value of 1% is equal to the experimental error of the discoloration measurements. Fig. 4 shows the time evolution of the residual concentration of MB under UV light irradiation, where C is the concentration of MB after the irradiation and C_0 is the starting concentration of MB. We tested the MB in the absence of any photocatalyst materials (squares), and in the presence of ZnO films with different thickness (circles for 9 nm, up triangles for 20 nm, diamonds for 31 nm, down triangles for 42 nm). No response was obtained without any sample, as expected; the ZnO films instead induced a significant degradation of MB. The analysis clearly indicates the dependence of the photocatalytic activity with the film thickness. The increase of the photo-activity with the film thickness is a consequence of more charge carriers generated by photo-absorption, but also of the enhanced crystallinity of the films detected by XRD analyses (see Fig. 2). It is worth noting that the photo-activity does not change significantly for films thicker than ~20 nm. This means that for thick films the charge carriers generated deeper than ~20 nm from the surface do not reach the surface, i.e. they recombine before reaching the surface, and as a consequence they do not contribute to the photoreactions.

After the photocatalytic test, the sample thicknesses were measured again by the ellipsometer, in order to check the eventual corrosion of the ZnO during the photocatalytic process [19]. The measurements did not reveal any difference in the film thickness, confirming the absence of any photo-corrosion phenomenon.

According to the Langmuir-Hinshelwood model, the photo-degradation reaction rate (k) of water contaminants is given by the following equation:

$$\ln \frac{C}{C_0} = -kt \tag{3}$$

where t is the irradiation time [20]. Therefore, it was possible, by a simple fitting procedure, to extract the MB photo-degradation reaction rates for the different ZnO films.

The photo-activity strongly depends on the bulk transport of the charge carriers to the surface of the ZnO films. Many papers reported on carrier lifetime in ZnO, in order to clarify the material quality and device performance (see for example Ref. [1]), while to our knowledge no one experimentally established the diffusion length of charge carriers in ZnO. Here we report an approach previously applied for TiO_2 films [21]. This approach enables separating surface from bulk effects in describing the photocatalytic activity of films, by investigating the effect of the film thickness on the photo-activity. Since the surface properties are the same for any film thickness of the same material, any change in the photo-activity can be solely ascribed to the increased bulk volume. The increase in the photocatalytic activity with the film thickness is thus a consequence of more charge carriers generated by photo-absorption in the bulk reaching the surface. This photo-activity-increase saturates for films that are thicker than the layer that gives charges for surface reaction, i.e., when the film becomes thicker than the maximum charge diffusion length [21]. Consequently, this approach applied to ZnO films allowed to indirectly measure the surface region that contributes to the photocatalytic reactions, i.e., the diffusion length of charge carriers in ZnO layers. Fig. 5 reports (with circles) the measured reaction rate, k, as a function of the film thickness for ZnO films deposited at 80 °C. The maximum activity is reached for ~20 nm thick film. In order to quantify the charge diffusion length, normal to the surface, we fitted the increase in photocatalytic activity with increasing film thickness by an exponential dependence [21]:

$$k = D\left(1 - e^{-\frac{d}{\lambda}}\right) \tag{4}$$

where k is the measured decomposition rate constant, d is the film thickness. D and λ are the fitting parameters, where D corresponds to the activity for very thick films. The best fit gives a value for λ of 10.7 ± 0.7 nm. The parameter λ may be interpreted as the charge diffusion length (normal to the surface), and its value indicates the distance from the surface at which a generated charge carrier has a probability *1/e* to reach the surface. This investigation demonstrated the importance of the film thickness and should be taken into account for the production of more efficient ZnO-based photocatalyst.

Different deposition temperatures were tested besides 80 °C: 40 and 120 °C. The growth rates were estimated by measuring the thickness of thin films grown on Si (depositing for each temperature three samples with different thickness, i.e. with different cycles). The experimental results are reported in Fig. 6 as a function of the deposition temperature. The error in the evaluation of the growth rate came from the thickness measurements and it is within the symbols, for this reason the errors are invisible in the graphic. The observed trend is in good agreement with what reported in literature [10]. We wish to underline that the growth window of ZnO ALD process ranges from 100 to 180 °C [10]; as a consequence, for the lowest investigate temperatures (i.e. 40 and 80 °C) we operated away from the ALD window, observing however a great repeatability of the deposition processes, in terms of the deposited thicknesses.

Once the growth rates for the three different temperatures (40, 80, and 120 °C) were estimated, we investigated the effect of the deposition temperature on the photo-activity of the films, by fixing the thickness. The thickness was set at 20 nm, since this thickness was demonstrated to maximize the photocatalytic response at 80 °C (see Figs. 4 and 5).

The surface morphology of three films, 20 nm thick, deposited at 40, 80 and 120 °C was investigated by SEM analyses in plan-view. The SEM images of the ZnO films are reported in Fig. 8. The images indicate some differences in the film structure. The deposition provided surfaces with small grains, uniformly distributed, with a size decreasing with the temperature, in good agreement with what reported in the literature [10].

The crystallinity of the three films, 20 nm thick, deposited at 40, 80 and 120 °C was investigated by XRD. The spectra are reported in Fig. 8. All the films were polycrystalline with the wurtzite structure. The good structural quality of the ZnO film deposited at 40 °C was quite an unexpected feature. Indeed, it was generally assumed that LT deposition should give amorphous films. In contrast, we found that our LT-ALD deposition recipe is able to grow polycrystalline Zn even at 40 °C. A more in-depth observation of the XRD patterns indicates that the relative intensity of the individual peaks strongly depends on the deposition temperature. We observed that the (002) crystallographic orientation, i.e. the situation where the *c*-axis is perpendicular to the layer surface, is dominant at low temperature (40 and 80 °C). On the other hand, at the deposition temperature of 120 °C the (100) crystallographic orientation, i.e. the situation where the *c*-axis is parallel to the layer surface, becomes equally important. Thus, the substrate temperature has a profound impact on the crystal orientation, which evolves from the (002) direction to the (100) and (101) one.

Fig. 9 shows the photocatalytic activity of the ZnO films, 20 nm thick, deposited at different temperatures tested towards the degradation of MB dye. We tested the MB in the absence of any photocatalyst materials (squares), and in the presence of ZnO films, 20 nm thick, deposited at different temperatures (circles for 40 °C, up triangles for 80 °C, down triangles for 120 °C). No response was obtained without any samples in contact with the MB solution, as expected; the ZnO films instead induced a significant degradation of MB. The analysis indicated an anomalous trend of the photocatalytic activity with the deposition temperature. In detail, the photocatalytic performance improves from 40 to 80 °C, and worsens at 120 °C. On the contrary, we would have expected a further improvement of the photo-activity due to the higher deposition temperature. The reason for this worsening can be explained by the crystallographic orientation of the ALD films. Indeed, the (001) facets lead to a significant enhancement of the photocatalytic activity [22,23]. Therefore, since at 120 °C the preferential orientation along the (002) is lost in favour of the (100), as reported in Fig. 7, this sample showed a deterioration of its photocatalytic performance (down triangles in Fig. 8) with respect to the photocatalytic response of the sample deposited at 80 °C. Therefore, the best sample, in terms of photo-activity, was the ZnO film 20 nm thick deposited at 80 °C.

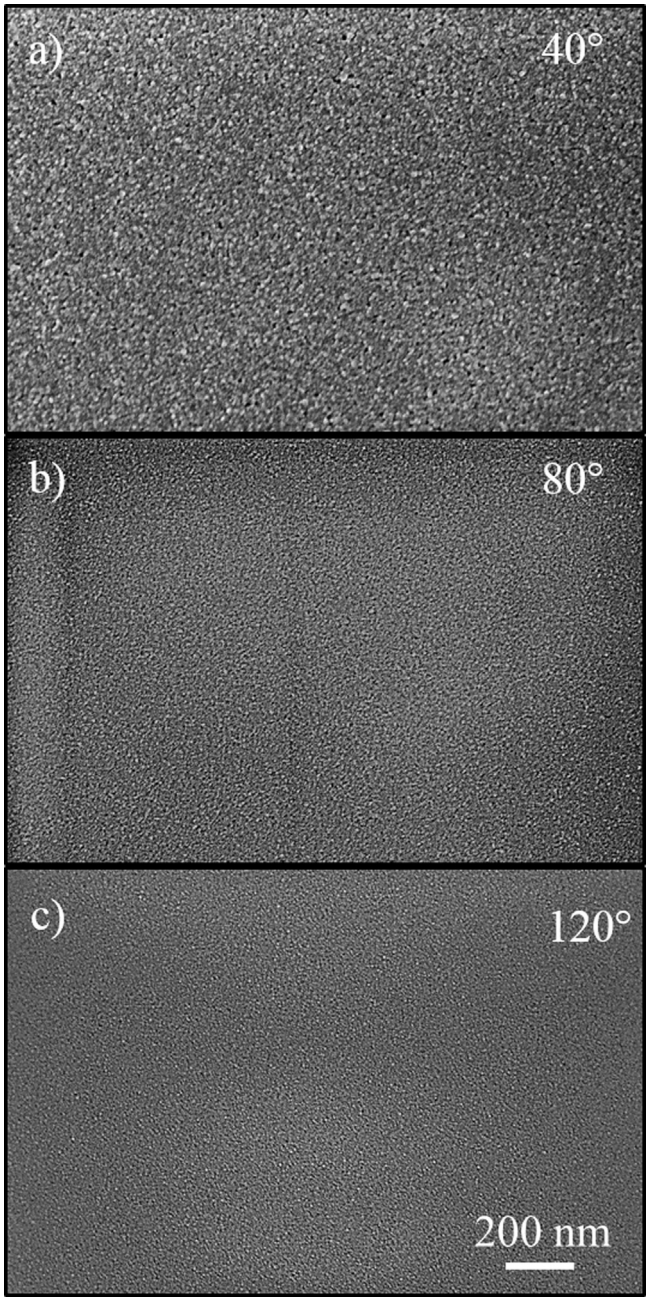

Fig. 7. Plan-view SEM analyses of ZnO thin, film 20 nm thick, deposited at 40 °C (a), 80 °C (b), or 120 °C (c).

Once the film thickness (~20 nm) and the deposition temperature (80 °C) were optimized, we transferred the LT-ALD process on a flexible support. The PEN polyester was chosen and used as substrate, due to its suitable thermal properties (glass transition temperature ~150 °C), chemical resistance, and high barrier to oxygen transmission. These properties have made PEN appealing, in particular, for bottling beverages that are susceptible to oxidation, such as beer and citrus juices. So, in view of a possible application of ZnO for water treatment, PEN support appears as an excellent candidate. It is worth noting that the absence of chemical groups (i.e. hydroxyl groups) on the polymer surface can hinder the ALD film growth [24]. Wilson et al., proposed a model for Al_2O_3 ALD

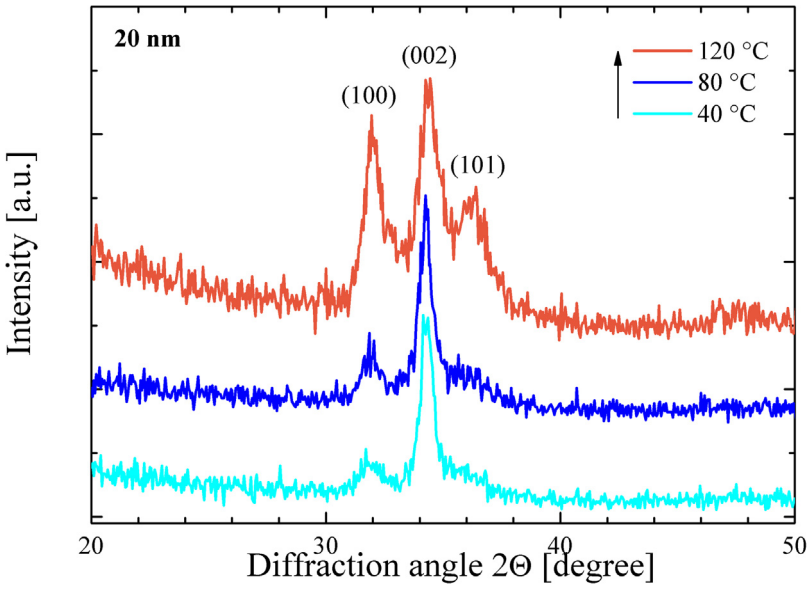

Fig. 8. XRD patterns of ZnO films, 20 nm thick, deposited by ALD at 40, 80, or 120 °C.

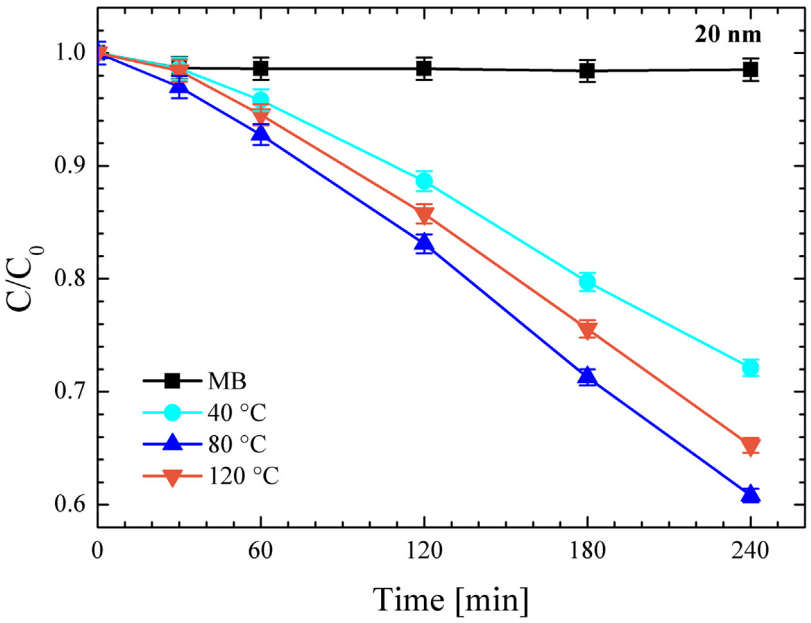

Fig. 9. MB photo-degradation under UV irradiation for four samples: MB (squares), MB with the ZnO films 20 nm thick deposited at: 40 °C (circles), 80 °C (up triangles), or 120 °C (down triangles).

nucleation and growth on polymers [25]. This model predicts the Al_2O_3 ALD growth without specific chemical species react with Tri-Methyl Aluminium, TMA (i.e., the first precursor). The nucleation of Al_2O_3 ALD is facilitated by TMA diffusion into the polymers and the subsequent reaction of the retained TMA with H_2O (i.e., the second precursor). Despite the interest on polymers for various application, few groups investigated the ALD on polymer films, and no one reported the ZnO ALD on PEN.

After a careful process optimization we obtained a ZnO film on PEN of ~50 nm. The ZnO thickness on PEN substrate was estimated by the focused ion beam (FIB) technique, with a Zeiss X-Beam 1550 equipment. The sample was, first of all, covered with a layer of gold (~250 nm in thickness) by sputtering. Afterwards, it was cut with the Ga^+ ion beam, and then observed in cross-view with the electron beam. Fig. 10 reports the SEM analysis of the sample. From the bottom the PEN substrate, the ZnO film and the Au coating can be easily detected. The ZnO film follows the morphology of the polymer, and it resulted ~50 nm in thickness. The thickness of ZnO simultaneously deposited on Si substrate was 48 nm by ellipsometry, in perfect agreement with the thickness deposited on PEN. For low film thickness PEN instead resulted to be an inhibitor for the ZnO growth. In the case of a process growing a 20 nm film (corresponding to 220 ALD cycles) on Si, there was no detectable film growth on PEN. After this onset, the growth rate proceeds faster than on Si substrate, so to obtain after 500 cycles the same ZnO thickness irrespective of the substrate. This peculiar behaviour was already observed for ZnO grown by ALD on PMMA (polymethyl methacrylate), polystyrene, and octadecylsilane monolayers [26].

The photocatalytic activity of the ZnO film on PEN was tested by the degradation of MB, and reported in Fig. 11. Four samples were tested: MB without any photocatalyst immersed (squares), MB with PEN (closed circles), MB with ZnO film deposited on PEN

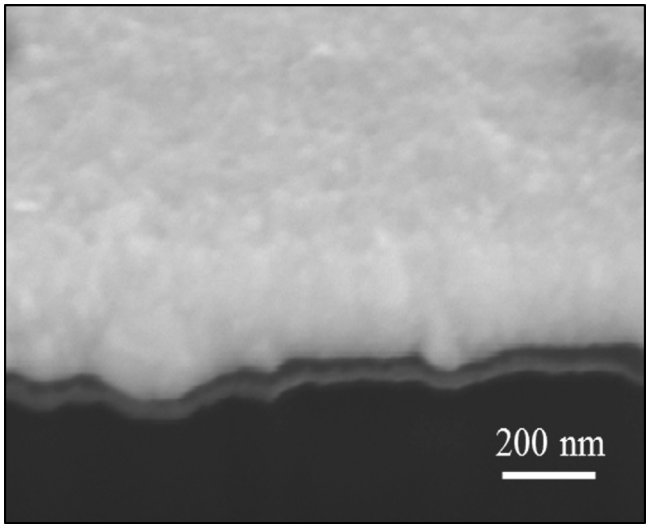

Fig. 10. Cross-view SEM analyses of ZnO thin deposited at 80 °C on PEN.

(open circles), MB with ZnO deposited on Si (triangles). The MB solution and the MB with PEN did not show any degradation of MB, as expected; on the other hand the two ZnO films showed a significant reduction of MB, irrespective of the substrates. In particular, we observed the degradation of ~30% of MB by the ZnO films after 4 h.

In order to demonstrate that the synthesized material is also active in the degradation of dangerous organic pollutants, the photo-degradative performance of ZnO films deposited on PEN was evaluated in terms of phenols degradation. Phenols are toxic and water refractory pollutants hardly degraded through common wastewater treatment methods. Fig. 12 reports the percentage of the phenol degradation after 240 min of irradiation under UV light. The photocatalytic response of the ZnO films was compared to the response of the phenol solution without any catalyst materials ("blank" on the abscissa axis of Fig. 12), and with a piece of PEN, as a reference. The two reference samples (i.e. "blank" and PEN) showed a negligible degradation of phenols (within the 2%), as expected. Instead, the thin films of ZnO deposited on PEN or on Si were able to remove ~30% of phenols present in the solution. The small difference in the phenol degradation between the ZnO films deposited on PEN and on Si is in our opinion ascribable to experimental errors.

4. Conclusions

In summary, we synthesized several ZnO thin films by low temperature (from 40 to 120 °C) ALD technique. XRD analyses proved the polycrystalline structure of the ZnO films, even for the samples deposited at 40 °C, despite the low deposition temperature. The photocatalytic activity of the materials was investigated, by the MB degradation, as a function of the film thickness and the deposition temperature. We found that for ZnO films deposited at 80 °C a surface region of ~20 nm contributes the charge carriers to the photoreactions. The trend of the photocatalytic activity with the deposition temperature appeared strongly dependent on the crystallographic orientation of the films. In particular, the samples deposited at 80 °C showed the best photocatalytic performance, since the (002) orientation prevails. Finally, we fabricated flexible photocatalytic films by depositing by ALD at 80 °C a thin film of ZnO on PEN. The films showed a significant efficiency in the photodegradation of MB and phenols in water. These results demonstrate that the LT-ALD can be employed as a simple method to produce functional flexible films that can found applications in photocatalysis, for example for water purification or water splitting, but also in sensors, photonics, and electronics.

Acknowledgements

The authors wish to thank Giuseppe Pantè (CNR-IMM) for technical assistance. We thank Domenico Mello for the FIB-SEM analysis, performed using the facilities of STMicroelectronics of Catania. This work has been supported by the FP7 European Project WATER (Grant Agreement 316082).

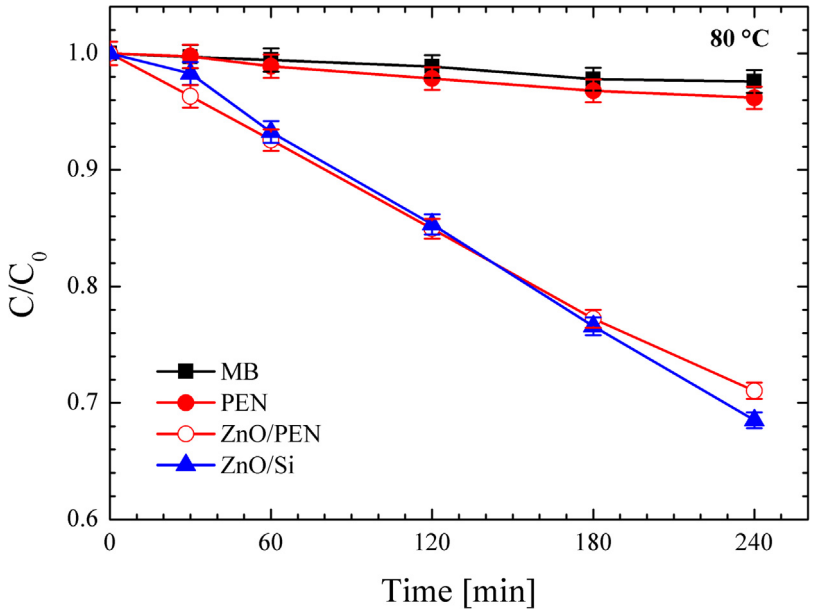

Fig. 11. MB photo-degradation under UV irradiation for four samples: MB (squares), MB with the PEN (closed circles), MB with ZnO film deposited on PEN (open circles), MB with ZnO film deposited on Si (triangles).

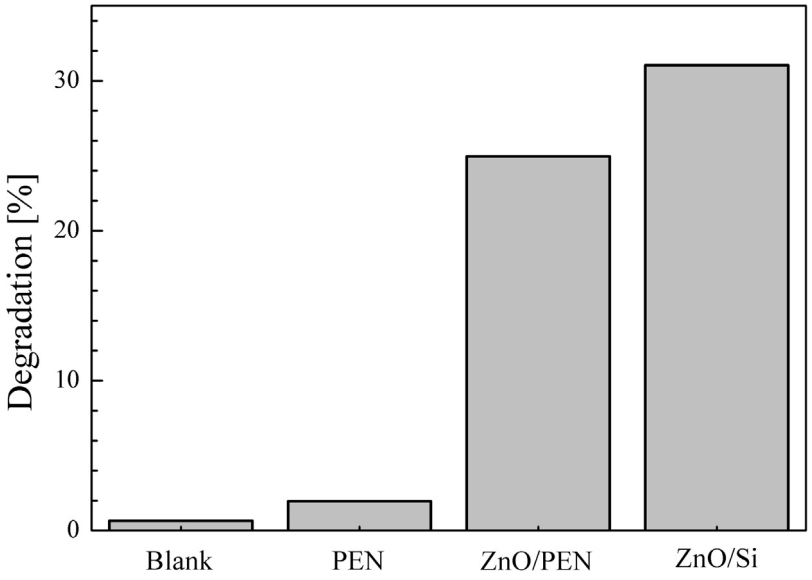

Fig. 12. Phenol photo-degradation in the absence of the catalyst (blank), and for different investigated samples: PEN, ZnO deposited on PEN (ZnO/PEN), and ZnO deposited on Si (ZnO/Si), both deposited at 80 °C.

References

[1] Ü. Özgür, I. Ya. Alivov, C. Liu, A. Teke, M.A. Reshchikov, S. Doan, V. Avrutin, S.J. Cho, H. Morkoç, J. Appl. Phys. 98 (041301) (2005) 1–303.
[2] D.-J. Lee, H.-M. Kim, J.-Y. Kwon, H. Choi, S.-H. Kim, K.B. Kim, Adv. Funct. Mater. 21 (2011) 448–455.
[3] I. Udom, M.K. Ram, E.K. Stefanakos, A.F. Hepp, D.Y. Goswami, Mater. Sci. Semicond. Process. 16 (2013) 2070–2083.
[4] K.U. Iwu, V. Strano, A. Di Mauro, G. Impellizzeri, S. Mirabella, Cryst. Growth Des. 15 (2015) 4206–4212.
[5] A. Di Mauro, M. Zimbone, M. Scuderi, G. Nicotra, M.E. Fragalà, G. Impellizzeri, Nanoscale Res. Lett. 10 (484) (2015) 1–7.
[6] S. Masuda, K. Kitamura, Y. Okumura, S.J. Miyatake, Appl. Phys. 93 (2003) 1624–1630.
[7] P.F. Carcia, R.S. McLean, M.H. Reilly, G. Nunes Jr., Appl. Phys. Lett. 82 (2003) 1117–1119.
[8] M. Ritala, J. Niinistö, ECS Trans. 25 (2009) 641–652.
[9] V. Lujala, J. Skarp, M. Tammenmaa, T. Suntola, Appl. Surf. Sci. 82/83 (1994) 34–40.
[10] E. Guziewicz, I.A. Kowalik, M. Godlewski, K. Kopalko, V. Osinniy, A. Wójcik, S. Yatsunenko, E. Łusakowska, W. Paszkowicz, M.J. Guziewicz,Appl. Phys. 103 (2008), 033515 1–6.
[11] P.C. Rowlette, C.G. Allen, O.B. Bromley, A.E. Dubetz, C.A. Wolden, Chem. Vap. Deposition 15 (2009) 15–20.
[12] M. Vähä-Nissi, M. Pitkänen, E. Salo, E. Kenttä, A. Tanskanen, T. Sajavaara, M. Putkonen, J. Sievänen, A. Sneck, M. Rättö, M. Karppinen, A. Harlin, Thin Solid Films 562 (2014) 331–337.
[13] D.A. Keane, K.G. McGuigan, P. Fernández Ibáñez, M.I. Polo-López, J.A. Byrne, P.S.M. Dunlop, K. O'Shea, D.D. Dionysiouf, S.C. Pillai, Catal. Sci. Technol. 4 (2014) 1211–1216.
[14] R. Wang, K. Hashimoto, A. Fujishima, M. Chikuni, E. Kojima, A. Kitamura, M. Shimohigoshi, T. Watanabe, Nature 388 (1997) 431–432.
[15] Compendium of chemical terminology, in: A.D. McNaught, A. Wilkinson (Eds.), The Gold Book, 2nd edn, Blackwell Scientific Publications, Oxford, 1997.
[16] F. Solís-Pomar, E. Martínez, M.F. Meléndrez, E. Pérez-Tijerina, Nanoscale Res. Lett. 6 (524) (2011) 1–11.
[17] J. Tauc (Ed.), Amorphous and Liquid Semiconductors, Plenum, New York, 1974, pp. 172–178.
[18] B.D. Viezbicke, S. Patel, B.E. Davis, D.P. Birnie III, Phys. Status Solidi B 8 (2015) 1700–1710.
[19] Y.-Q. Cao, J. Chen, H. Zhou, L. Zhu, X. Li, Z.-Y. Cao, D. Wu, A.-D. Li,Nanotechnology 26 (2015), 024002 1–9.
[20] M.N. Chong, B. Jin, C.W.K. Chow, C. Saint, Water Res. 44 (2010) 2997–3027.
[21] T. Luttrell, S. Halpegamage, J. Tao, A. Kramer, E. Sutter, M. Batzill, Sci. Rep. 4 (4043) (2014) 1–8.
[22] E.S. Jang, J.-H. Won, S.-J. Hwang, J.-H. Choy, Adv. Mater. 18 (2006) 3309–3312.
[23] J.H. Zeng, B.B. Jin, Y.F. Wang, Chem. Phys. Lett. 472 (2009) 90–95.
[24] N. Pinna, M. Knez (Eds.), Atomic Layer Deposition of Nanostructured Materials, Wiley-VCH, Weinheim, Germany, 2012, pp. 201–203.
[25] C.A. Wilson, R.K. Grubbs, S.M. George, Chem. Mater. 17 (2005) 5625–5634.
[26] D.H. Levy, S.F. Nelson, D.J. Freeman, Display Technol. 5 (2009) 484–494.